Renewable Energy, Environment, and Power Quality Journal (REE&PQJ)
ISSN:3020-531X
Volume 24, January 2026

Inductive Wireless Power Transfer for Autonomous Underwater Vehicles using Split Core Transformer and Resonant LLC Circuit

Iñigo Rozas, Iñigo Martínez de Alegría, Alberto Otero, Endika Robles and Iker Aretxabaleta

Applied Electronics Research Team (APERT), University of the Basque Country (UPV/EHU)
Bilbao School of Engineering, 48013 Bilbao (Spain)

Phone number: +34 946013915

Abstract.

Unmanned Underwater Vehicles (UUVs) are pivotal for underwater exploration and maintenance. Autonomous Underwater Vehicles (AUVs), with their potential to reduce operational time and environmental impact, are gaining increased interest. However, they face important technological challenges, particularly in power supply. This study focuses into the application of Inductive Wireless Power Transfer (IWPT) for continuous AUV operation, employing tightly coupled split core transformers (SCT) designed for near-field power transfer. Robust isolation and alignment mechanisms are proposed to overcome the effects of seawater environment. An IWPT device with an SCT and resonant LLC circuit is simulated and experimentally tested. Finite Element Method studies highlight the advantage of isolating the device from the seawater environment, especially at high frequencies. LLC simulation and experimental results demonstrate an efficiency in power transfer of 93.2 % and 87.1 %, respectively, transferring up to 312 W. However, global efficiency of the experimental device drops to 76.4 %, highlighting the need for optimizations in circuit design.

Keywords.

Inductive Wireless Power Transfer, Autonomous Underwater Vehicles, Resonant Converters, Finite Element Analysis.

1. Introduction.

Unmanned Underwater Vehicles (UUVs), including remotely operated vehicles (ROVs) and autonomous underwater vehicles (AUVs), play an important role in several underwater exploration, observation, and maintenance tasks. This extends to the inspection and maintenance of marine energy infrastructures such as offshore wind farms, tidal and wave energy plants [1]. ROVs are generally the main option for offshore maintenance tasks. However, their need for on-site operation from vessels and the limited weather windows for operations are leading the industry to view AUVs as a promising alternative. By adopting autonomous solutions, technicians' time in offshore parks can be reduced, leading to benefits such as greater operational availability, reduced pollution from vessels and accident minimization.

However, AUVs face various technological challenges, with power supply being a key concern. Typically reliant on batteries, enabling underwater charging stations would ensure their continuous operation. Inductive wireless power transfer (IWPT) stands out as a notable technology under investigation for charging these devices. Many recent studies have focused on this technology, and several proposals have been presented [2]. In this work, tightly coupled split core transformers (SCT) are examined for their potential to enhance coupling, minimize losses in ionized seawater, and operate effectively as regular, low-regulated high-frequency transformers.

2. IWPT system overview.

In recent years, the application of inductive wireless power transfer techniques has seen significant growth, especially in sectors like mobile charging, healthcare, and electric vehicles. There are established commercial standards for inductive wireless power, such as the Qi standard from the Wireless Power Consortium (WPC) for planar wireless charging technology devices [3].

IWPT systems rely on the principle of transferring electrical energy wirelessly between two coils, typically referred to as the transmitter (Tx) and receiver (Rx). These coils are generally resonated with a capacitance tuned to the desired resonant frequency [4]. These coils and capacitances form the resonant tank as presented in Fig. 1. The system input converters transform the AC or DC electric power from sources like marine renewables into high-frequency AC, by controlling the switching of an inverter. This resonant power, excites the Tx coil, generating a time-varying magnetic field. The power is transmitted to the receiver and then, the output converters transform the AC into DC to charge the battery.

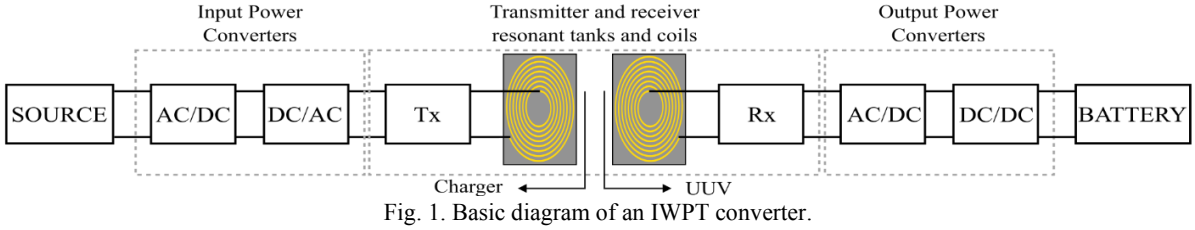

Fig. 1. Basic diagram of an IWPT converter.

3. IWPT prototype design considerations.

A. General coil design considerations.

The coil design is essential in any IWPT application, as it will determine the efficiency of the power transfer. Initially, its operating field needs to be determined. Depending on the distance, systems can operate in the near-field or far-field regions [4]. In this study, near-field operation is chosen to enhance magnetic coupling. The geometric shape of the coil and core material significantly affects magnetic field distribution and efficiency. Circular coils are commonly used (Fig. 2a), but other shapes like rectangular or elliptical are also employed [2]. Additionally, incorporating a highly permeable ferrite core can improve the magnetic coupling [4]. This core must be designed so it does not reach its saturation current.

$$I_{sat} = \frac{(B_{sat} \cdot A_e)}{\sqrt{(A_L \cdot L)}} [A] \quad (1)$$

Where I_{sat} is the saturation current, B_{sat} is the saturation flux (T), A_e core effective area (m^2), L the inductance (H) and A_L the inductance per turns^2 ($\frac{H}{N^2}$)

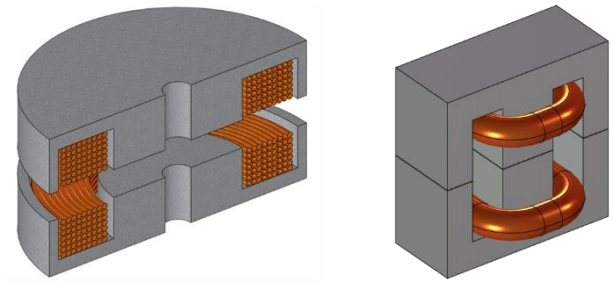

a) b)

Fig. 2. a) Planar circular coils. b) Split core transformer.

In this study, the less-explored E-shaped core paired with a circular coil is evaluated for its suitability and potential to optimize power transfer efficiency. The selected coil configuration, depicted in Fig. 2.b, is a single-turn split core transformer (SCT) designed for near-field operation.

B. Underwater Design Considerations.

In underwater IWPT systems, radiation and eddy current losses (ECL) are primary concerns affecting efficiency. These losses, influenced by coil design and operating frequencies, become significant at higher frequencies and longer distances as portrayed in Fig. 3. However, at frequencies below 200kHz, power transfer remains largely unaffected for tightly coupled systems [5], [6]. Nonetheless, higher frequencies generally allow using compact devices with a higher power density.

The dynamic nature of sea currents can cause misalignment between T_x and R_x sides, reducing their coupling and overall efficiency. Moreover, biofouling can further interfere with coil performance [7]. Although specific coil designs aim to mitigate misalignments and biofouling challenges [8], [9], alternative solutions, including mechanical devices or isolating chambers, are underexplored. The experimental prototype is designed with the assumption that it will require robust isolation and alignment to overcome these challenges.

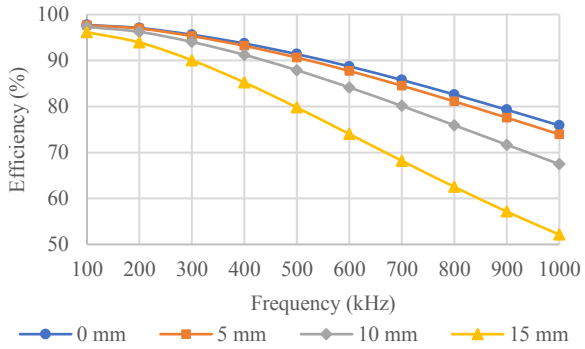

Fig. 3. WPT efficiency for several f values and distances [6].

In seawater, communication signals can also be significantly attenuated, making reliable communication challenging. Given the dynamic nature of seawater and these communication constraints, there is a growing emphasis on control methods that can maintain maximum efficiency without direct communication links between sides [10], [11]. To address these challenges, efforts are directed towards developing robust designs that minimize the need for communication-based control mechanisms, enhancing overall resilience.

Lastly, high pressures of deeper ocean regions require robust equipment designs. Such pressures can potentially alter the permeability of materials like ferrite cores [12]. This alteration might compromise magnetic shielding and escalate radiation losses.

C. Resonant Tank Topologies.

Resonant compensation topologies play a crucial role in wireless power transfer. These configurations are typically classified by the arrangement of compensating capacitors and inductors employed, as well as their specific configurations. Among the prevalent configurations in wireless power transfer systems are Series-Series (SS), Series-Parallel (SP), Parallel-Parallel (PP), and Parallel-Series (PS). SP and SS topologies are generally chosen for enhanced power transfer with SS being appropriate for lower load conditions and SP for higher loads [13].

A novel approach to further improve IWPT, involves combining series and parallel topologies to achieve enhanced power transfer [14], [15]. A single inductor, along with series and parallel capacitors, forms an LCC configuration topology. This features the possibility of incorporating more resonant frequencies, but it requires two large and independent capacitors due to high AC currents. Another topology is LLC, which is composed by a series resonant inductance (L_r) and capacitance (C_r) and the transformer's magnetizing inductance (L_m). It has the advantage of integrating the two physical inductors into a single component. The LLC converter in Fig. 4.a, with a half bridge inverter and diode bridge rectifier is the configuration selected for this study.

4. LLC Topology Overview.

A. *Characteristics of LLC converters.*

LLC converters find widespread applications in various fields, notably in renewable energy systems, electric vehicles, and server power supplies [16]. However, the application of LLC converters UWPT is not a broadly studied topic due to concerns about misalignment, which can compromise their efficiency. These converters are typically optimized for constant output and frequency, and any variation in these parameters can lead to decreased performance. Nonetheless, ensuring proper alignment, especially in AUVs, can mitigate this issue.

LLC converters offer reliable power transfer due to their robustness, with the added benefit of enabling control without direct transmitter-receiver communication. These converter offers several advantages in terms of handling a wide range of input voltages, soft-switching operation, and power density [15]. Additionally, the converter utilizes soft-switching techniques, such as zero-voltage switching (ZVS) and zero-current switching (ZCS), which minimize switching losses and improves efficiency. However, its implementation may involve higher costs and design complexity compared to other converter topologies [15].

B. *FHA study in LLC converters.*

To characterize resonant tanks, the First Harmonic Approximation (FHA) is employed, simplifying the analysis by filtering out harmonics. The FHA assumes that only the first harmonic significantly contributes to current flow, facilitating the development of converter equations without significantly compromising accuracy [17]. The resonance frequency is calculated for the fundamental wave. The resonance frequency for an LLC converter is:

$$f_r = \frac{1}{2\pi\sqrt{L_r C_r}} \ [Hz] \tag{2}$$

FHA methods allows the control of magnitudes by adjusting the resonance frequency. This method is particularly useful in deriving the transfer function or gain equation of the converter. Before modelling the circuit, it's essential to define variables like the inductance ratio (m):

$$m = \frac{L_m}{L_r} \tag{3}$$

The reflected load resistance:

$$R_e = \frac{8}{\pi^2} \cdot \frac{{N_p}^2}{{N_s}^2} \cdot R_{out} \tag{3}$$

Where N_p is primary turns, N_s secondary turns of the transformer. The load quality factor (Q_e):

$$Q_e = \frac{\sqrt{L_r/C_r}}{R_e} \tag{4}$$

The normalized operating frequency (f_n):

$$f_n = \frac{f_{sw}}{f_r} \tag{5}$$

Where f_{sw} is the switching frequency of the device.

Based on these definitions and the equations derived from [18], the LLC converter's voltage gain expression can be formulated as follows:

$$G(f_n, m, Q_e) = \frac{1}{\sqrt{\left(1 + m - \frac{m}{{f_n}^2}\right) + {Q_e}^2 \cdot \left(f_n - \frac{1}{f_n}\right)^2}} \tag{6}$$

From this gain expression, the following gain curves can be obtained for any device:

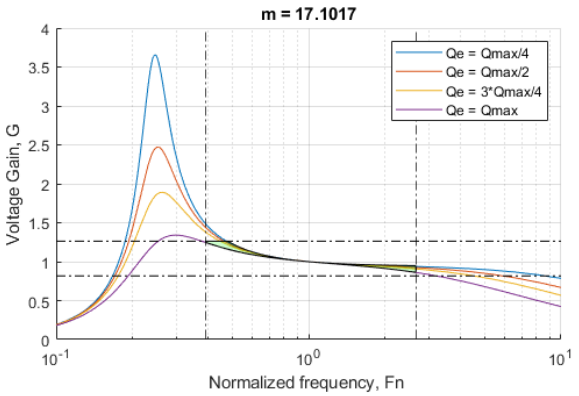

Fig. 5. Gain curves for chosen LLC prototype.

The device should always operate within the green area and, optimally, at the resonant frequency (f_n), ensuring correct operation and the maintenance of the required voltage output within the given input voltage range.

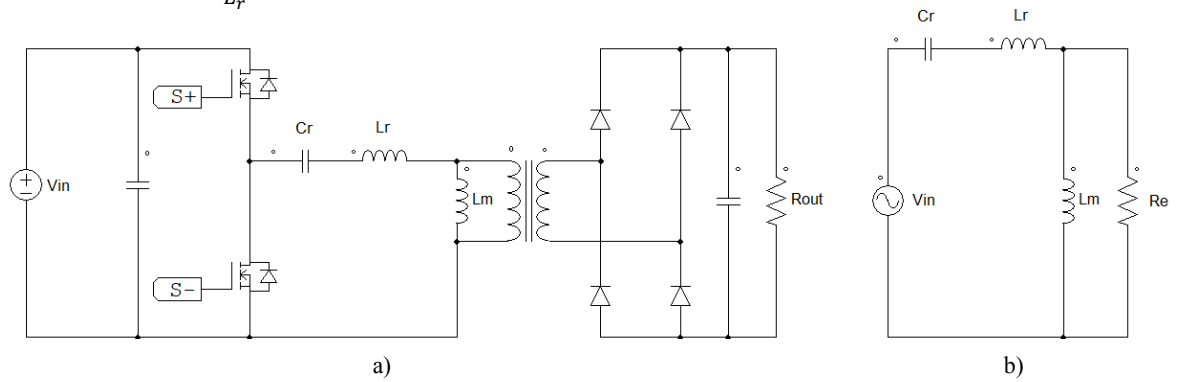

a) b)

Fig. 4. a) LLC converter with half-bridge inverter and diode bridge rectifier. b) FHA equivalent circuit of an LLC converter.

5. Simulations and Finite Element Analysis.

A. FEM Studies.

The SCT was modeled using finite element methods (FEM) to assess the potential effects of seawater. The device was tested inside an air recipient and in contact with seawater at various frequency values in a 3D magnetic field study. The targeted power output was set to 1 kW.

Table I. Parameter definition of model materials.

Parameter	Seawater	Air	Copper	Ferrite
Relative permeability	1	1	1	2000
Relative permittivity	80	1	1	1
Conductivity (S/m)	5.5	$6 \cdot 10^{-7}$	$6 \cdot 10^{7}$	10^{-6}

For this study, a frequency sweep from 100 kHz to 1000 kHz in steps of 100 kHz was conducted, and the input and output power were calculated. The resonant capacitor was changed to be resonated for each frequency. Additionally, graphical results of the volumetric loss density and magnetic flux density were computed. Figures 6 and 7 present these results for a frequency value of 500 kHz.

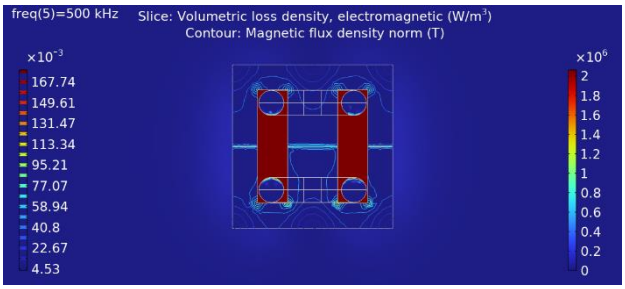

Fig. 6. 3D magnetic study of SCT in seawater for 500kHz.

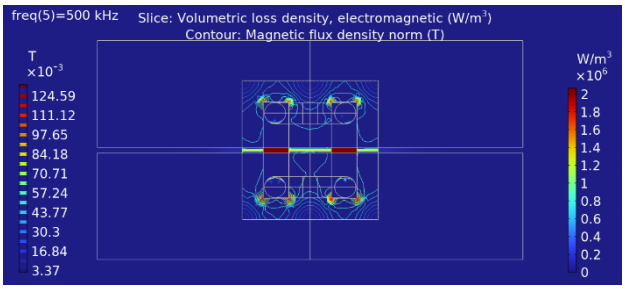

Fig. 7. 3D magnetic study of SCT in air recipient for 500kHz.

Additionally, based on the obtained power values, the efficiency for both tests is presented in Fig. 8.

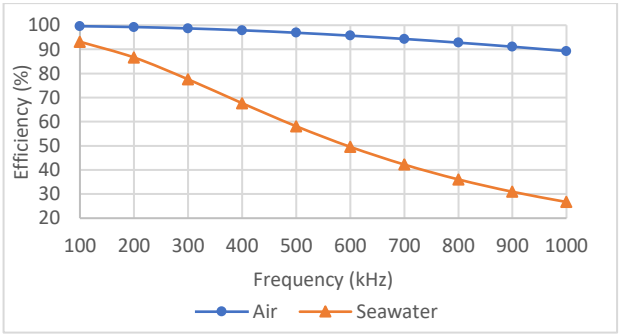

Fig. 8. Power values for the SCT in air and seawater.

As observed in Fig. 8, efficiency decreases with frequency; however, when the device is introduced into the recipient air, its efficiency significantly improves. Figures 6 and 7 reveal that volumetric loss density is high only in areas where the device is in contact with water, attributed to ECL and radiation losses, and it also rises with frequency. Additionally, it is important to note that the magnetic flux density is maintained below 0.3 T for all frequency values, adhering to the standard saturation value for ferrite materials. This indicates that the materials are suitable for power transfer up to 1 kW. In this case, a frequency of around 100 kHz is chosen for the prototype. Nevertheless, for miniaturization, this frequency could be increased until a compromise is achieved between size and power density, provided the device is properly isolated.

B. Electronic circuit simulation

The resonant circuit depicted in Fig. 4.a is the chosen design. It incorporates a half-bridge inverter at the input and a full-bridge rectifier at the output. Fig. 5. displays the gain curves for the device. The circuit utilizes parameters derived from actual values measured on the real SCT.

Table II. Parameters of simulated LLC converter.

Parameter	Value
V_{in}	56 V
f_r	100 kHz
C_r	4.293 µF
L_m	9.5 µH
L_r	0.59 µH
R_{trafo}	0.1 Ω
R_{out}	2 Ω
C_{filt}	100 µF

As suggested by the results from Fig. 8 no additional losses were introduced due to the seawater environment, considering the device is situated inside a recipient. The duty cycle of the device was configured to 0.5 with a short deadtime period of 0.1 µs. The following curves were obtained in PSIM:

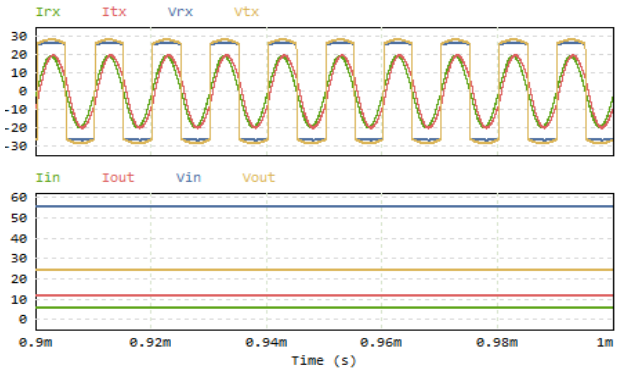

Fig. 9. Voltage and Current curves of simulated LLC converter.

The power transfer is not ideal, as the model's resistance was set to the measured value in the real transformer. The voltage was halved since the input converter is a half-bridge inverter and the current was multiplied. However, non-ideally set switches and diodes caused additional reduction in the output voltage and current values. The objective in this scenario was to achieve an output similar to 24 V, a standard value for Li-Ion batteries.

6. Experimental test.

As previously stated, the prototype's frequency was fixed at 100 kHz, and the experiment took place in air. The SCT functions in the near field as a transformer, featuring one turn on each side. The input voltage was adjusted to 60 V.

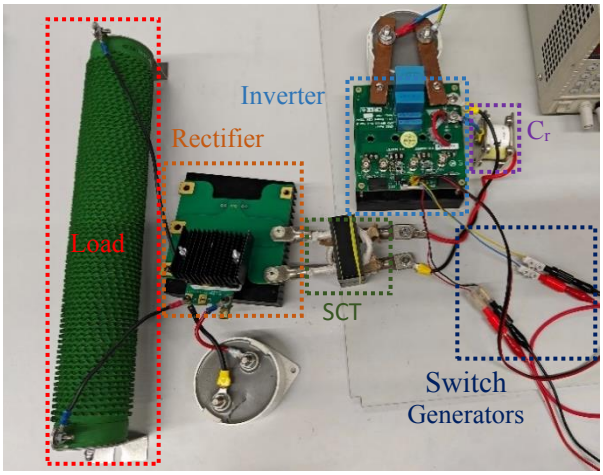

Fig. 11. Experimental setup of the prototype.

Certain parameters of the converter needed tuning, primarily due to the introduction of undesired inductances from parallel cables or the partly inductive load. The resonant capacitance was chosen to be 2.4 µF, and rather than the theoretical 134 kHz resonance according to equation (2), the actual resonance occurred at 96 kHz. After testing the device with the specified input voltage and frequency values, the oscilloscope captured the following curves.

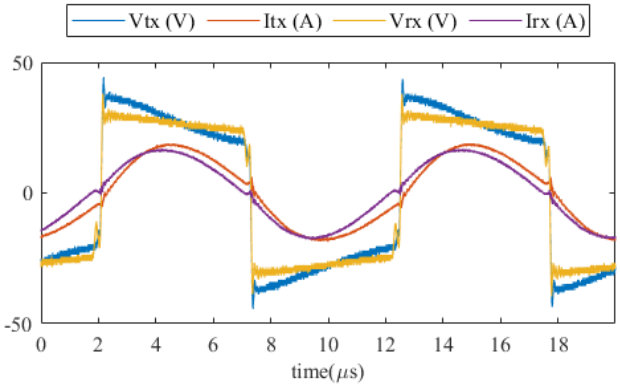

Fig. 10. Tx and Rx values from oscilloscope.

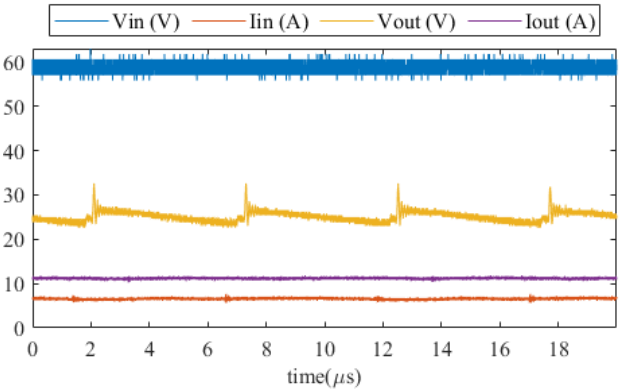

From these results and the simulations, the following power and efficiency table is built:

Table III. Power and efficiency results.

Parameter	Simulation	Experiment
P_{in}	345.8 W	371 W
P_{Tx} (RMS)	343.8 W	359.3 W
P_{Rx} (RMS)	320.9 W	313 W
P_{out}	304.9 W	283.4 W
WPT Efficiency	93.3 %	87.1 %
Global Efficiency	88.2 %	76.4 %

In both scenarios, the WPT efficiency demonstrates high performance, with the simulation achieving 93.3%, with a slightly lower value during the experiment at 87.1%. However, the global efficiency drops from 88.2%, to 76.4% in the experiment. The efficiency reduction observed during the experiment can be attributed to loss sources, such as parallel cables or inefficient switches and diodes. To enhance efficiency, future improvements could involve optimizing and compacting PCB designs and minimizing these loss sources.

7. Conclusions.

This study explores the application of Inductive Wireless Power Transfer for enhancing the continuous operation of AUVs by addressing power supply challenges. The utilization of tightly coupled split core transformers designed for near-field power transfer, coupled with robust isolation and alignment mechanisms, demonstrates a promising approach. FEM studies underscore the advantages of isolating the device from the harsh seawater environment, particularly at high frequencies. ECL and radiation losses are highly reduced in this case, and saturation is not reached for power values around 1 kW.

The simulation and experimental testing of an IWPT device incorporating SCT and resonant LLC circuit reveal notable results. The power transfer efficiency achieved in both simulation (93.2%) and experiments (87.1%) show consistency for a WPT of 312 W. However, the observed drop in global efficiency to 76.4% in the experimental device highlights the necessity for further improvements in the circuit design. Optimization is crucial for achieving a more consistent and reliable performance of the IWPT system for powering AUVs in real-world applications. Future studies should incorporate efficiency control methods that do not require communication between Tx and Rx sides for the device to function optimally. Moreover, tests with a battery are required to verify the actual efficiency during charging.

Despite these challenges, the study underscores the potential of tightly coupled and highly isolated IWPT as a viable solution for overcoming power supply limitations in underwater environments and emphasizes the importance of ongoing research and development in this domain. Ensuring an efficient, clean, and safe power supply for AUVs would enhance the sustainability of inspection and maintenance activities for offshore installations, including marine energy power plants.

Acknowledgements

This work was supported in part by the Government of the Basque Country within the fund for research groups of the Basque University system IT1440-22 and by the CIN/AEI/10.13039/501100011033 within the project PID2020- 115126RB-I00. This work was supported in part by “Programa Investigo” within the European Union funding framework of NextGenerationEU.

References.

[1] A. Sahoo, S. K. Dwivedy and P. S. Robi, "Advancements in the field of autonomous underwater vehicle," *Ocean Eng.,* vol. 181, pp. 145-160, 2019.

[2] C. R. Teeneti *et al*, "Review of Wireless Charging Systems for Autonomous Underwater Vehicles," *IEEE J. Ocean. Eng.,* vol. 46, *(1),* pp. 68-87, 2021.

[3] W. Zhong, D. Xu and R. S. Y. Hui, *Wireless Power Transfer between Distance and Efficiency.* Springer, 2020.

[4] M. Etemadrezaei, "22 - wireless power transfer," in *Power Electronics Handbook (Fourth Edition)*, M. H. Rashid, Ed. 2018,

[5] T. Orekan, P. Zhang and C. Shih, "Analysis, Design, and Maximum Power-Efficiency Tracking for Undersea Wireless Power Transfer," *IEEE Journal of Emerging and Selected Topics in Power Electronics,* vol. 6, *(2),* pp. 843-854, 2018.

[6] I. Rozas Holgado *et al*, "Wireless Power Transfer: Underwater loss analysis for different topologies and frequency values," *Proceedings of the IECON 2020 Conference,* pp. 3942-3947, 2020.

[7] J. Oiler *et al*, "Thermal and biofouling effects on underwater wireless power transfer," *Proceedings of the 2015 IEEE Wireless Power Transfer Conference, WPTC 2015,* pp. 1-4, 2015.

[8] C. Cai *et al*, "A Misalignment Tolerance and Lightweight Wireless Charging System via Reconfigurable Capacitive Coupling for Unmanned Aerial Vehicle Applications," *IEEE Transactions on Power Electronics,* vol. 38, *(1),* pp. 22-26, 2023.

[9] S. Niu *et al*, "Underwater Wireless Charging System of Unmanned Surface Vehicles with High Power, Large Misalignment Tolerance and Light Weight: Analysis, Design and Optimization," *Energies,* vol. 15, *(24),* pp. 1-19, 2022.

[10] L. Kang, Y. Hu and W. Zheng, "Maximum power efficiency tracking on underwater magnetic resonant wireless power transfer system," *Harbin Gongcheng Daxue Xuebao/Journal of Harbin Engineering University,* vol. 38, *(6),* pp. 829-835, 2017.

[11] Z. Zheng, N. Wang and S. Ahmed, "Maximum efficiency tracking control of underwater wireless power transfer system using artificial neural networks," *Proceedings of the Institution of Mechanical Engineers.Part I: Journal of Systems and Control Engineering,* vol. 235, *(10),* pp. 1819-1829, 2021.

[12] Z. Li *et al*, "Design considerations for electromagnetic couplers in contactless power transmission systems for deep-sea applications," *Journal of Zhejiang University SCIENCE C,* vol. 11, *(10),* pp. 824-834, 2010.

[13] D. B. Ahire, V. J. Gond and J. J. Chopade, "Compensation topologies for wireless power transmission system in medical implant applications: A review," *Biosensors and Bioelectronics: X,* vol. 11, pp. 1-10, 2022.

[14] B. Zhang *et al*, "A wireless power transfer system for an autonomous underwater vehicle based on lightweight universal variable ring-shaped magnetic coupling," *International Journal of Circuit Theory and Applications,* pp. 1-20, 2023.

[15] S. -. Wu and C. -. Han, "Design and Implementation of a Full-Bridge LLC Converter with Wireless Power Transfer for Dual Mode Output Load," *IEEE Access,* vol. 9, pp. 120392-120406, 2021.

[16] J. Zeng *et al*, "LLC resonant converter topologies and industrial applications — A review," *Chinese Journal of Electrical Engineering,* vol. 6, *(3),* pp. 73-84, 2020.

[17] J. Deng *et al*, "Design Methodology of LLC Resonant Converters for Electric Vehicle Battery Chargers," *IEEE Transactions on Vehicular Technology,* vol. 63, *(4),* pp. 1581-1592, 2014.

[18] S. De Simone *et al*, "Design-oriented steady-state analysis of LLC resonant converters based on FHA," in 2006.